

1 Transformation of char carbon during bubbling fluidized bed gasification of biomass

2 Kevin J. Timmer^{a, 1} and Robert C. Brown^b

3 ^a (Corresponding author), Black Engineering, Iowa State University, Ames, IA 50011, USA; e-mail:

4 Kevin.Timmer@dordt.edu; Declaration of Interests: None

5 ^b Center for Sustainable Environmental Technologies, Iowa State University, 1140 BRL, Ames, IA
6 50011, USA; e-mail: rcbrown3@iastate.edu; Declaration of Interests: None

7 **Abstract**

8 This study focuses on the fate of carbon in the char generated by devolatilization of biomass during
9 fluidized bed gasification. A carbon balance model was developed to distinguish between char
10 transformed to carbon-bearing gases and its comminution and elutriation as fine char during gasification.
11 The model accurately predicts the transient accumulation of char carbon in the reactor. Experiments
12 revealed steady state reactor char carbon loadings were achieved after multiple hours of gasification. The
13 model formed the basis of an experimental methodology that assesses the transformation of char carbon
14 based on collection of elutriated solids from the reactor and assessment of the steady state char carbon
15 loading in the reactor. Experiments were performed to distinguish the relative contributions of chemical
16 reaction and physical comminution toward conversion of char to gaseous and solid products. The effects
17 of equivalence ratio, gasification temperature, superficial gas velocity, biomass particle size, and the
18 addition of steam on the partitioning of char carbon between gaseous and solid products during
19 gasification of ground seed corn in a bubbling fluidized bed were investigated. This study revealed that
20 char conversion during gasification of biomass was limited by elutriation of fine char particles arising
21 from fragmentation or attrition of primary char product. Additionally, increased chemical reaction of char
22 to form gases was usually accompanied by increased elutriation of fine char, which suggests that chemical
23 reaction increased the porosity of the char and its susceptibility to fragmentation and attrition. Finally,
24 decreasing superficial gas velocity, increasing equivalence ratio, and decreasing particle size led to
25 increased carbon conversion, while increasing temperature and steam concentration in the reactor had
26 negligible effect.

27 Keywords: biomass gasification; carbon balance; fluidized bed; char conversion; comminution;
28 chemically enhanced attrition

29 ¹ Present address: 498 4th Ave NE, Sioux Center, IA 51250, USA; e-mail: Kevin.Timmer@dordt.edu

30

31 **1. Introduction**

32 The physical and chemical processes that control the partitioning of carbon between gas and solid
33 products during biomass gasification are not well understood. Gasification of biomass in a fluidized bed
34 reactor is often limited by incomplete conversion of char to carbon-bearing gases due to loss through
35 comminution to fine particles that elutriate from the reactor. Equilibrium thermodynamic calculations
36 [1]–[8] indicate that carbon in char should be completely transformed into gases at typical gasification
37 operating conditions, but most biomass gasifiers produce significant char co-product [1], [9]–[30].

38 The overall yield of carbon-bearing gases is defined as the fraction of the fuel carbon that is converted
39 to gas, vapor, or aerosol form. A majority of the biomass carbon leaves the reactor transformed as carbon
40 monoxide (CO), carbon dioxide (CO₂), methane (CH₄), and elutriable char with smaller contributions
41 from other light hydrocarbons and tar (condensable organic compounds).

42 Efforts to improve the yield of carbon-bearing gases from char have focused on enhancing gas-solid
43 reactions of oxygen and steam with char. Yield of these gases increases with increasing equivalence ratio
44 (ER) [1], [9], [11]–[15], [21], [23], [28]. However, increasing ER beyond an optimum level lowers the
45 caloric content of the produced gas [1], [7], [10], [11], [21], [24], [28], [31], [32]. Attempts to improve
46 the yield of carbon in the gaseous products leaving fluidized bed gasifiers through addition of steam [12],
47 [20], [21], [24], [30] or operation at higher temperatures [1], [9], [11], [13], [14], [16]–[22], [30] have met
48 with limited success.

49 The study of carbon conversion to gaseous products during fluidized bed gasification is complicated
50 by the fact that char carbon undergoes both chemical reaction and physical comminution.

51 Devolatilization of biomass and gas-solid reactions of char contribute to production of carbonaceous
52 gases while fragmentation and elutriation of char reduce gas yield. Carbon balances on fluidized beds
53 must account for these different forms of carbon. The goal of the present study was to measure char

54 conversion during fluidized bed gasification and relate it to important operating parameters including
55 equivalence ratio, reaction temperature, superficial gas velocity, biomass particle size, and the addition of
56 steam. Towards this end, a carbon balance model was developed to distinguish between char transformed
57 to carbon-bearing gases and its comminution and elutriation as fine char during gasification. This model
58 was used to analyze experimental data obtained from a laboratory-scale fluidized bed gasifier and
59 determine rates of transformation of char to gas or attrition to elutriable fines as a function of operating
60 conditions.

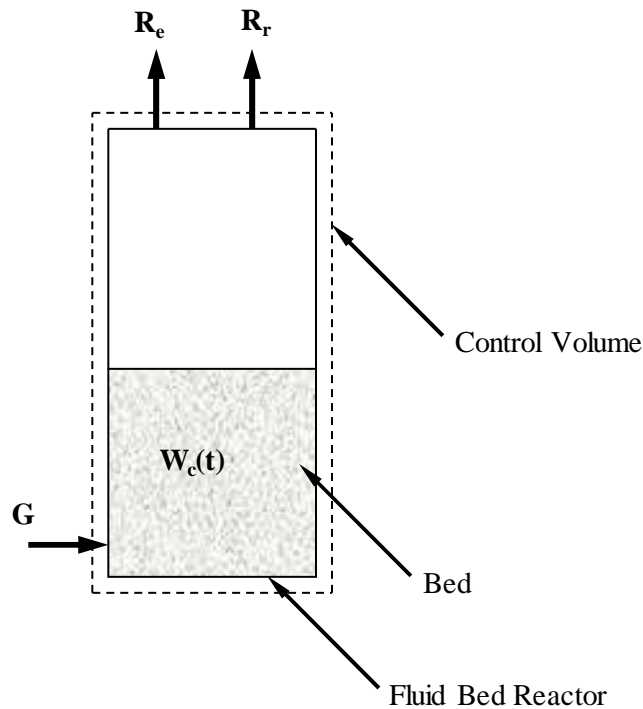
61 **2. Theory and calculations**

62 A carbon balance model was devised to distinguish between char conversion to carbon-bearing gases
63 and its comminution and elutriation as fine solids. Char carbon is defined as residual solid carbon
64 remaining after devolatilization of biomass in the fluidized bed. This is different from fixed carbon
65 determined by ASTM proximate analysis (ASTM Standard E 870-82). The amount of carbon remaining
66 in the char after devolatilization of biomass depends on particle temperature and heating rate [27], [29],
67 [32]–[45], which are likely to be different during fluidized bed gasification than the conditions of ASTM
68 proximate analysis.

69 As illustrated in Figure 1, the rate of accumulation of char carbon in the reactor, dW_c/dt , is the sum of
70 the rate at which it is generated by devolatilization of biomass, G ; the rate that it is elutriated as fine solid
71 from the gasifier, R_e ; and the rate at which it is converted to carbon-bearing gases due to chemical
72 reaction, R_r :

$$73 \quad \frac{dW_c}{dt} = G - R_e - R_r \quad (1)$$

74



W_c = char carbon loading in the reactor (g)

G = char carbon generation rate (g/s)

R_e = char carbon elutriation rate (g/s)

R_r = char carbon chemical reaction rate (g/s)

75
76
77
78

Figure 1. Control volume used for determining the mass balance of char carbon during biomass gasification

79

The char carbon generation rate due to biomass devolatilization, G , is a function of the feed rate of biomass into the gasifier, F , and the fraction of biomass that is converted into char carbon, f_c :

81

$$G = f_c F \quad (2)$$

82

As subsequently demonstrated by experiment, f_c is a function of devolatilization temperature.

83

During operation at fixed conditions the elutriation rate is proportional to the mass of char carbon in the reactor [46], [47]:

85

$$R_e = k_e W_c \quad (3)$$

86

where k_e (s^{-1}) is the char carbon elutriation rate coefficient.

87

The chemical reaction rate is assumed to be first order with respect to the amount of char carbon

88

present:

89
$$R_r = k_r W_c \quad (4)$$

90 where k_r (s^{-1}) is the gas-solid chemical reaction rate coefficient.

91 The total char carbon removal rate (R_t) from the gasifier is the sum of the removal rates by chemical
92 reaction and elutriation:

93
$$R_t = k_e W_c + k_r W_c = k_t W_c \quad (5)$$

94 where k_t is the total char carbon removal rate coefficient. Substituting Eq. (5) into Eq. (1) gives:

95
$$\frac{dW_c}{dt} = G - k_t W_c \quad (6)$$

96 While gasifying under fixed operating conditions, including temperature, k_e , k_r , and k_t are expected to
97 remain essentially constant. Therefore, separating variables and integrating yields:

98
$$W_c(t) = \frac{G}{k_t} [1 - \exp(-k_t t)] \quad (7)$$

99 which predicts the mass of char carbon in the reactor at any time, t . At large times ($t = t_{ss}$) a steady state
100 carbon loading in the reactor, $W_c(t_{ss})$, is approached. At steady state, Eq. (7) can be rearranged to:

101
$$k_t = \frac{G}{W_c(t_{ss})} \quad (8)$$

102 3. Material and methods

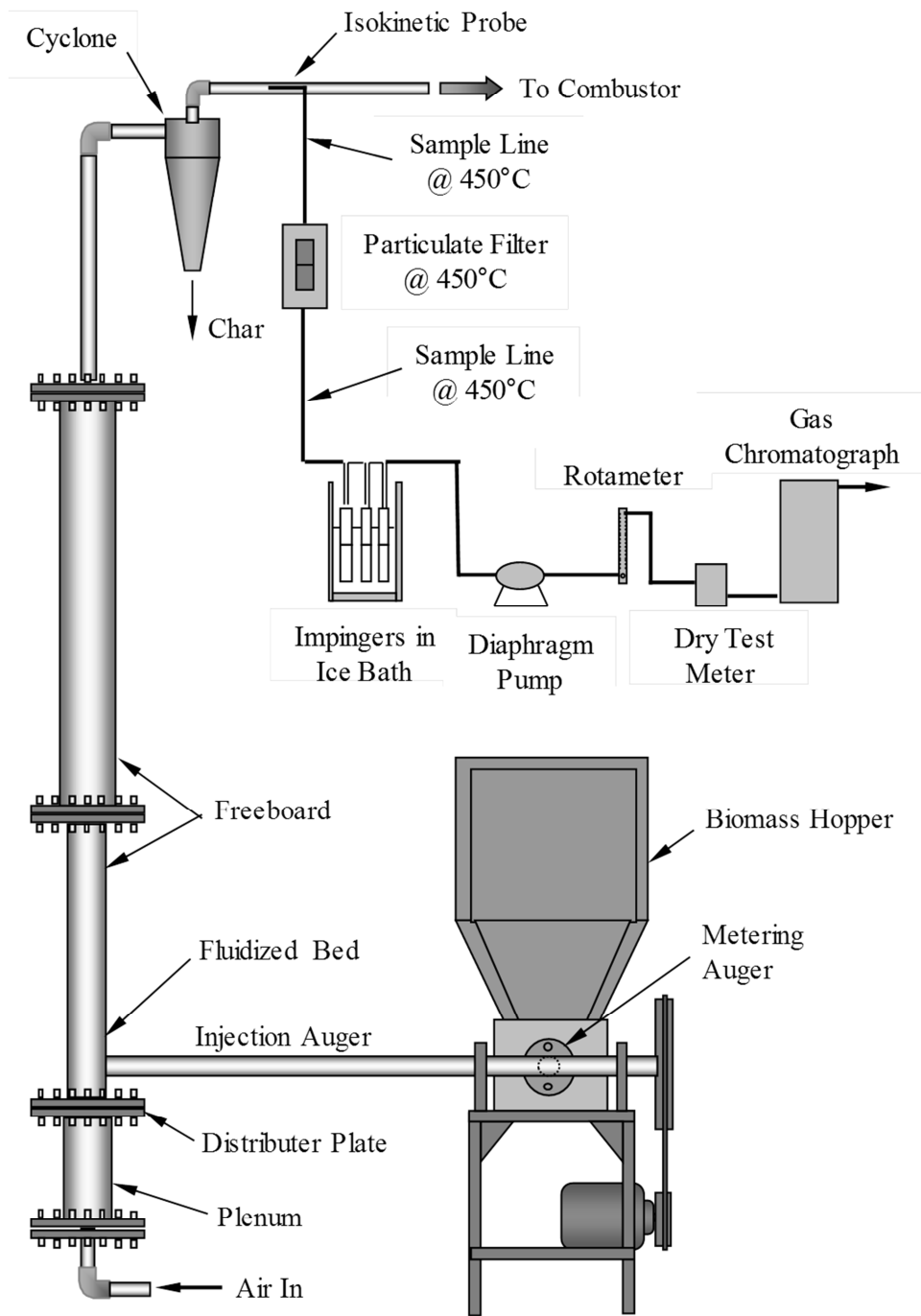
103 3.1 Gasifier and gas/char sampling system

104 Experiments were performed in a laboratory scale (10 kW_{th}) atmospheric bubbling fluidized bed
105 gasifier, illustrated in Figure 2. The flow of air into the reactor was controlled by a mass flow controller
106 and was preheated by a star-wound cable heater located in the plenum section. The main reaction
107 chamber was constructed of two flanged Inconel 625 pipes. The 9.53 cm diameter lower section was
108 81.3 cm long while the 15.2 cm diameter upper portion was 122 cm in length. Temperatures in the
109 reactor were controlled independent of ER with a series of high temperature semi-cylindrical ceramic
110 fiber guard heaters that encase the gasifier. The fluidization media consisted of a mixture of 70 wt%
111 silica sand with a mass weighted average diameter of 0.321 mm and 30 wt% calcined limestone of a total
112 mass of approximately 2000 g. The calcined limestone reacted with alkali released from the biomass to

113 mitigate against ash slagging and agglomeration of bed material [48], [49]. The minimum fluidization
114 velocity of the bed was measured to be 2.06 cm/s at 700°C. As shown in Figure 2, a precision metering
115 auger fed biomass from the hopper perpendicularly into a high speed injection auger connected to the
116 fluidized bed reactor.

117 The product gas stream from the gasifier exited through a cyclone particulate separator before being
118 sampled isokinetically. As illustrated in Figure 2, the gas sampling system consisted of a stainless steel
119 probe inserted in the gas flow, a heated quartz fiber thimble filter to collect particulate matter, an ice bath
120 impinger train to remove tar and water, a diaphragm vacuum pump to induce flow through the sampling
121 system, a rotameter and valve to adjust the gas flow appropriate to isokinetic sampling requirements, a
122 dry test meter to accurately measure the total flow volume over the course of an experiment, and a micro
123 gas chromatograph (GC) for measuring concentrations of N₂, O₂, H₂, CO, CO₂, C₂H₂, C₂H₄, and C₂H₆. To
124 prevent condensation of tar the temperature of the cyclone particulate separator, the exhaust piping, and a
125 portion of the sample system were maintained above 450°C with electrical resistance heating tape.

126 Discarded seed corn was employed as a model biomass fuel because it was easy to work with, fed
127 consistently, and its low ash content helped reduce the accumulation of alkali in the fluidized bed,
128 prolonging the bed's useful life. Table 1 gives the proximate and ultimate analysis of the ground seed
129 corn as reported by Hazen Research Inc., Golden, Colorado. The moisture content of the ground seed
130 corn varied between 11.2 – 13.1%, averaging 12.0% across the experiments. Whole kernel seed corn was
131 reduced using a portable agricultural feed grinder to two different particle size distributions. The coarse
132 grind produced particles with an average mass weighted diameter of 1.9 mm based on sieve data, while
133 the fine grind produced 0.96 mm diameter particles on average.



134
135

136 Figure 2. Schematic of gasifier with sample systems (note: for clarity ceramic guard heaters surrounding
137 the plenum, bed, and freeboard are not shown)
138

139

140

141

142 Table 1. Proximate and ultimate analysis of ground seed corn

	Biomass Component	Ground Seed Corn (% wt, dry)
Proximate	Volatile	86.44
	Fixed Carbon	11.77
	Ash	1.79
Ultimate	C	48.91
	H	5.95
	O	41.46
	N	1.73
	S	0.16
	Ash	1.79

143

144 *3.2 Experimental procedures*

145 *3.2.1 Biomass feed rate*

146 The ground seed corn was fed into the fluidized bed using a dual auger system as shown in Figure 2.
 147 At the conclusion of an experiment the average feed rate was calculated as the quantity of biomass
 148 gasified divided by the duration of the experiment.

149 *3.2.2 Steady state experiments*

150 Steady state experiments were performed at temperatures between 700 - 800°C and with ER values
 151 between 0.24 – 0.37. While steady temperatures in the reactor were typically achieved a few minutes
 152 after the biomass feed was initiated, true steady state gasification required establishment of the asymptotic
 153 char carbon loading in the unit, which required up to several hours of operation under some conditions
 154 (see Figure 4 for examples of carbon loading vs. time profiles).

155 Biomass feed rate was set to achieve the desired ER for the specified air flow rate. The ceramic
 156 guard heaters surrounding the reactor were used to control the temperature in the reactor independent of
 157 the ER value. The concentration of water vapor in the reactor was increased for some experiments by
 158 injecting wet steam into the bottom of the bed during gasification.

159 The steady state char carbon elutriation rate, $R_e(t_{ss})$ was determined using the cyclone catch and
 160 thimble filter catch. After establishing steady state gasification the cyclone catch can was removed and

161 replaced with a clean, pre-weighed catch can. Elutriated char was captured by the cyclone and collected
162 in the can over a measured length of time (typically 30 – 60 min) to give an adequate sample.
163 Concurrently, an isokinetic sample of the producer gas downstream of the cyclone was drawn through a
164 clean, pre-weighed quartz thimble filter. After the sampling period the cyclone catch and thimble filter
165 were recovered and weighed. The average residence time of the char carbon in the reactor was
166 sufficiently long in these experiments (20 – 70 min) to complete pyrolysis of the biomass [45]. Therefore
167 the collected char was assumed to be composed of carbon and ash. Consequently, the carbon content of
168 the cyclone catch and thimble filter catch was assessed as the mass lost after combustion in a bench top
169 furnace. The cyclone catch was used to estimate the mass of char carbon in the coarse particulate matter
170 leaving the gasifier. The thimble filter data was used in conjunction with the total volume of the
171 isokinetic gas sample to estimate the mass of char carbon in the fine particulate matter remaining in the
172 producer gas after passing through the cyclone. The steady state elutriation rate, $R_e(t_{ss})$, was calculated as
173 the sum of the fine and coarse char carbon collected divided by the sample time period. The total carbon
174 gas yield, Y_{tc} , is the fraction of carbon entering the reactor, both fixed and volatile, converted to a gas or
175 aerosol:

$$Y_{tc} = 1 - \frac{R_e(t_{ss})}{\dot{m}_{c,b}} \quad (9)$$

176
177 where $\dot{m}_{c,b}$ is the mass flow of carbon entering with the biomass, calculated as a product of the biomass
178 feed rate and the mass fraction of carbon in the biomass as given in Table 1. Note that this method of
179 calculating total carbon yield does not require measurement of the tar present in the product gas stream.

180 Experiments were concluded by “burning out the reactor” to determine the mass loading of char
181 carbon in the reactor during steady state operation, $W_c(t_{ss})$. Burnout was initiated by discontinuing the
182 biomass feed while maintaining the air flow. During burnout the flow of gaseous carbon leaving the
183 reactor was monitored using a micro GC to record the concentrations of the carbonaceous gases in the
184 product stream. The cyclone and thimble filters were used as describe previously in this section to
185 determine the quantity of char carbon that elutriated during burnout. Steady state char carbon loading in

186 the reactor was determined as the sum of the carbonaceous gas profiles integrated in time and the char
187 carbon elutriated during burnout.

188 Measurement of $R_e(t_{ss})$ and $W_c(t_{ss})$ allowed calculation of the elutriation rate coefficient by
189 rearrangement of Eq. (3):

$$k_e = \frac{R_e(t_{ss})}{W_c(t_{ss})} \quad (10)$$

191 The value of k_t was found using Eq. (8) and the chemical reaction rate coefficient, k_r , was calculated
192 by difference:

$$k_r = k_t - k_e. \quad (11)$$

194 Comparisons of k_e and k_r as a function of operating conditions shed light on how the char carbon
195 generated from the entering biomass was either transformed into a carbon-bearing gas or elutriated.

196 The gaseous carbon yield from char carbon, Y_{cc} , is defined as the fraction of the char carbon
197 generated from the biomass that is converted to a carbon-bearing gas and is given by:

$$Y_{cc} = 1 - \frac{R_e(t_{ss})}{G} \quad (12)$$

199 3.2.3 Char carbon fraction, f_c

200 The char carbon generation rate, G , was determined as a fraction of the total biomass feed rate (Eq.
201 (2)). The char carbon fraction, f_c , of ground seed corn was found experimentally as a function of
202 temperature by injecting 10 g batch samples of ground corn into the gasifier bed fluidized with N_2 and
203 held at temperature with the ceramic guard heaters for 30 minutes to ensure complete devolatilization.
204 After devolatilization of the sample, f_c was determined by burning the carbon out of the reactor,
205 integrating the carbon-bearing gas profiles in time, and combining that data with char carbon recovered
206 from the cyclone catch and thimble filter as described in *Section 3.2.2*.

207 3.2.4 Transient char carbon reactor loadings

208 Transient char carbon reactor loadings were measured to compare to model predictions (Eq. (7)).
209 Experiments were conducted by injecting biomass at constant rate into the pre-heated fluidized bed for
210 the desired length of gasification time. The experiment concluded by discontinuing biomass feed and

211 proceeding to burn out the reactor, while collecting elutriated char with the cyclone and thimble filters.
212 The char carbon loading was determined as described in *Section 3.2.2*.

213 *3.2.5 Uncertainty analysis*

214 The uncertainty in experimentally measured parameters was conservatively estimated based on the
215 limitations of the equipment and methodology employed and has been affirmed by replication of results.
216 The uncertainty in calculated values was estimated using error propagation methods [50]. Uncertainty
217 bars on data represent 95% confidence intervals. Note that in some instances the uncertainty bars are so
218 small as to be obscured by the data markers.

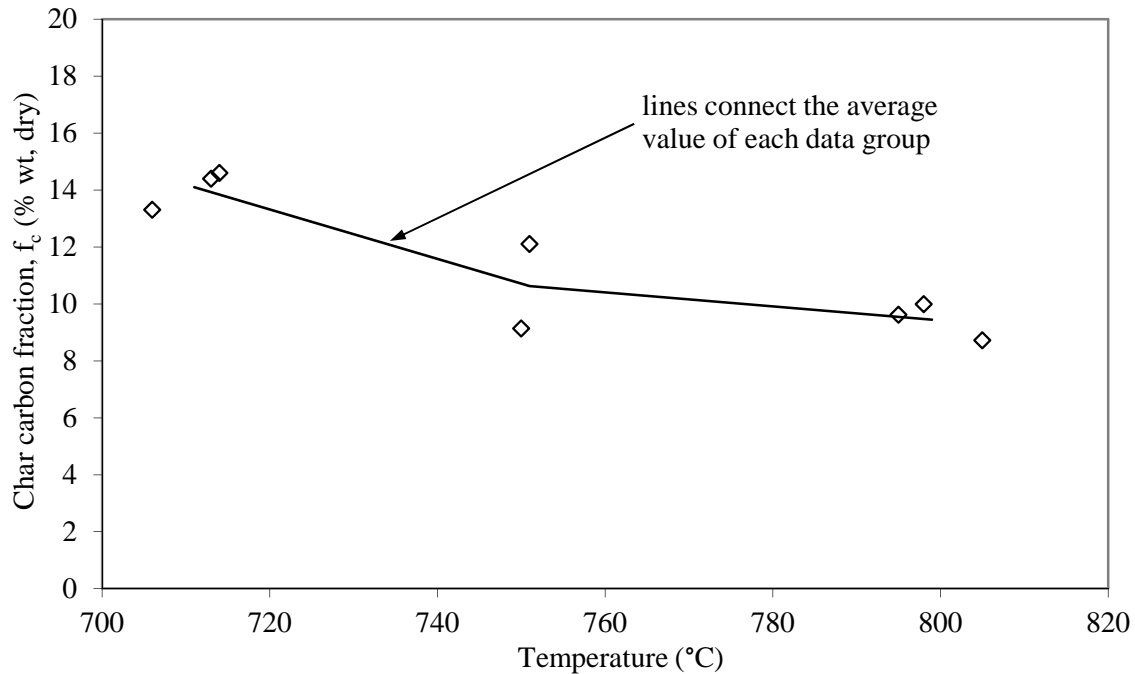
219 **4. Results and discussion**

220 *4.1 f_c vs. temperature*

221 The mass fraction of the biomass that remains as char carbon after devolatilization, f_c , depends on the
222 gasification temperature. The char carbon fraction as a function of temperature was measured for ground
223 seed corn using the method described in *Section 3.2.3*. The results of these experiments are given in
224 Figure 3. Lines connecting the average of each of the three groups of data have been added to help clarify
225 the relationship. The decreasing trend in the char carbon fraction with increasing temperature is
226 consistent with published results [27], [29], [32]–[45], [51]. It should also be noted that a proximate
227 analysis of the ground seed corn (Table 1) yielded a fixed carbon fraction of 11.77%, which is within the
228 range of the char carbon fractions measured here.

229 *4.2 Model validation*

230 The transient model of the char carbon loading in the reactor (Eq. (7)) was compared to experimental
231 results at two different operating conditions. A model was constructed for each operating condition by
232 calculating the char carbon generation rate using Eq. (2) and by experimentally measuring the steady state
233 carbon loading in the reactor, $W_c(t_{ss})$, as described in *Section 3.2.2*. These values were inserted into Eq.
234 (8), and then Eq. (7), to create the transient model. Transient char carbon loadings were measured
235 following the procedure described in *Section 3.2.4* by stopping gasification at specified times before
236 steady state conditions were achieved. The results of these experiments are given in Table 2.



237
 238 Figure 3. Char carbon fraction of devolatilized fine ground seed corn as a function of temperature.
 239 Gasifier was fluidized with nitrogen gas (ER = 0)
 240

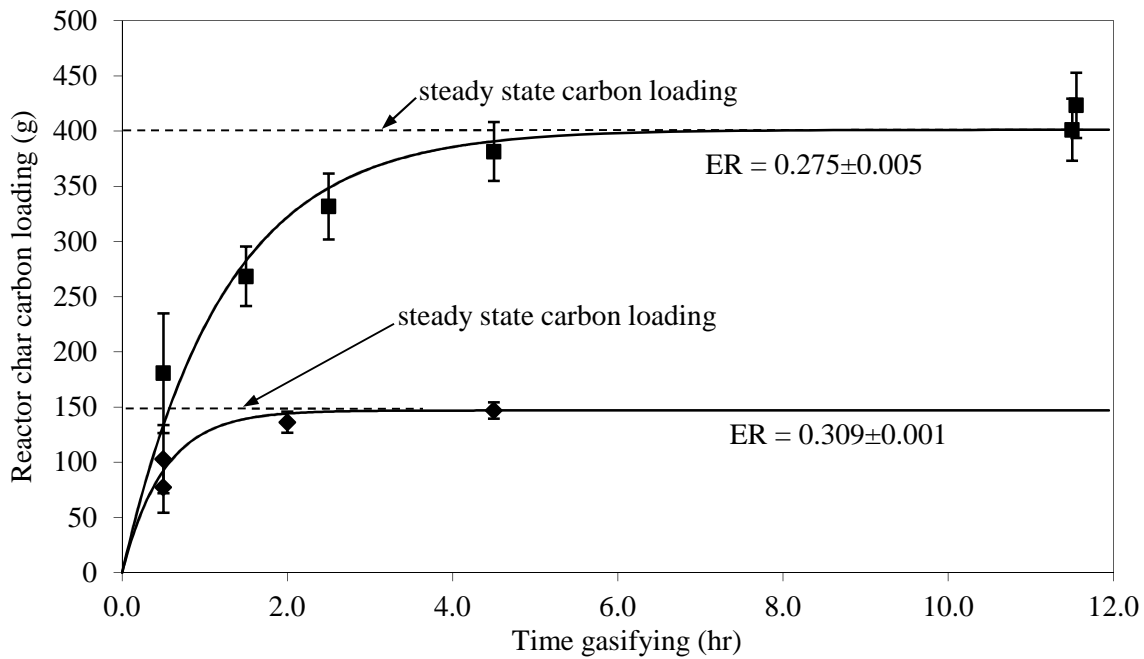
241 Figure 4 compares char carbon loadings in the fluidized bed vs. time for experiments (Experiments $a - j$)
 242 and model predictions (Eq. (7)) for gasification at 715°C and for two different equivalence ratios (ER =
 243 0.27 and ER = 0.31). The figure shows excellent agreement between the measured carbon loadings and
 244 those predicted by the model over time. The relatively large error bars at early times are due to
 245 uncertainty in the char carbon generation rate, G , caused by temperature fluctuations in the gasifier
 246 corresponding to the introduction of biomass into the preheated bed.

247 4.3 Steady state experiments

248 While the char carbon balance model accurately predicted the buildup of char carbon in the reactor
 249 over time (see Section 4.2), it was primarily used to analyze steady state experiments using the method
 250 described in Section 3.2.2. The char carbon analysis methodology was applied to measurements made
 251 during gasification of ground seed corn at various operating conditions. Table 2 shows the operating
 252 parameters for each of the steady state experiments in this study.

Table 2. Operating data and experimental results for gasification of ground seed corn

Exp.	Type	Time Gasifying	Feed Rate	Biomass Size	n_{H_2O}/n_{CC}	Air Flow	ER	Temp (°C)	f_c Figure 4 (%wt dry)	F (g/s)	W_c (g)	U_{fb} (cm/s)	R_e (10^{-3} g/s)	k_r (10^{-6} s $^{-1}$)	k_e (10^{-6} s $^{-1}$)	Y_{cc} (%)	Y_{tc} (%)
<i>a</i>	transient	0.50	0.594	Fine	0.6	50.0	0.309	715	13.7	0.0810	77	n/a	n/a	n/a	n/a	n/a	n/a
<i>b</i>	transient	0.50	0.594	Fine	0.6	50.0	0.309	715	13.7	0.0810	103	n/a	n/a	n/a	n/a	n/a	n/a
<i>c</i>	transient	2.00	0.594	Fine	0.6	50.0	0.309	715	13.7	0.0810	136	n/a	n/a	n/a	n/a	n/a	n/a
<i>d</i>	steady state	4.50	0.594	Fine	0.6	50.0	0.309	715	13.7	0.0810	147	n/a	n/a	n/a	n/a	n/a	n/a
<i>e</i>	transient	0.50	0.654	Fine	0.6	50.0	0.279	715	13.7	0.0942	181	n/a	n/a	n/a	n/a	n/a	n/a
<i>f</i>	transient	1.50	0.654	Fine	0.6	50.0	0.279	715	13.7	0.0942	268	n/a	n/a	n/a	n/a	n/a	n/a
<i>g</i>	transient	2.50	0.654	Fine	0.6	50.0	0.279	715	13.7	0.0942	332	n/a	n/a	n/a	n/a	n/a	n/a
<i>h</i>	transient	4.50	0.658	Fine	0.6	50.0	0.277	715	13.7	0.0942	381	n/a	n/a	n/a	n/a	n/a	n/a
<i>i</i>	steady state	11.50	0.673	Fine	0.6	50.0	0.271	715	13.7	0.0942	401	n/a	n/a	n/a	n/a	n/a	n/a
<i>j</i>	steady state	11.55	0.672	Fine	0.6	50.0	0.271	714	13.8	0.0928	423	28	12.2	190	28.8	86.8	96.3
<i>k</i>	steady state	4.75	0.535	Fine	0.8	40.0	0.273	748	10.8	0.0578	146	21	3.66	371	25.1	93.7	98.6
<i>l</i>	steady state	5.50	0.609	Fine	0.8	50.0	0.300	748	10.8	0.0658	164	28	5.26	368	32.0	92	98.2
<i>m</i>	steady state	3.48	1.061	Fine	0.8	83.0	0.286	750	10.6	0.1124	202	49	19.8	459	98.2	82.4	96.2
<i>n</i>	steady state	8.00	0.754	Fine	1.0	50.0	0.242	801	9.5	0.0716	198	38	13.4	295	67.7	81.3	96.4
<i>o</i>	steady state	6.75	0.678	Fine	1.0	50.0	0.269	801	9.5	0.0644	142	35	8.01	397	56.3	87.6	97.6
<i>p</i>	steady state	4.33	0.493	Fine	1.0	50.0	0.370	805	9.4	0.0464	71	30	4.39	587	61.4	90.5	98.2
<i>q</i>	steady state	7.25	0.689	Fine	0.9	50.0	0.265	751	10.5	0.0724	325	31	11.0	189	34.0	84.7	96.7
<i>r</i>	steady state	6.87	0.689	Fine	0.9	50.0	0.265	751	10.5	0.0724	318	31	11.3	192	35.6	84.3	96.6
<i>s</i>	steady state	7.42	0.652	Fine	0.9	50.0	0.280	753	10.5	0.0684	258	30	9.40	229	36.4	86.3	97
<i>t</i>	steady state	6.00	0.540	Fine	0.9	50.0	0.338	750	10.6	0.0572	136	28	6.56	373	48.3	88.5	97.5
<i>u</i>	steady state	6.00	0.518	Coarse	0.9	50.0	0.282	746	11.0	0.0570	224	26	10.4	209	46.4	81.8	95.9
<i>v</i>	steady state	4.83	0.677	Coarse	0.9	50.0	0.270	801	9.5	0.0643	144	34	13.9	350	96.5	78.4	95.8
<i>w</i>	steady state	3.50	0.739	Fine	1.8	50.0	0.247	798	9.5	0.0702	111	36	12.0	524	108.	82.9	96.7
<i>x</i>	steady state	3.25	0.724	Fine	2.9	50.0	0.252	797	9.5	0.0688	93	38	10.2	632	110.	85.2	97.1



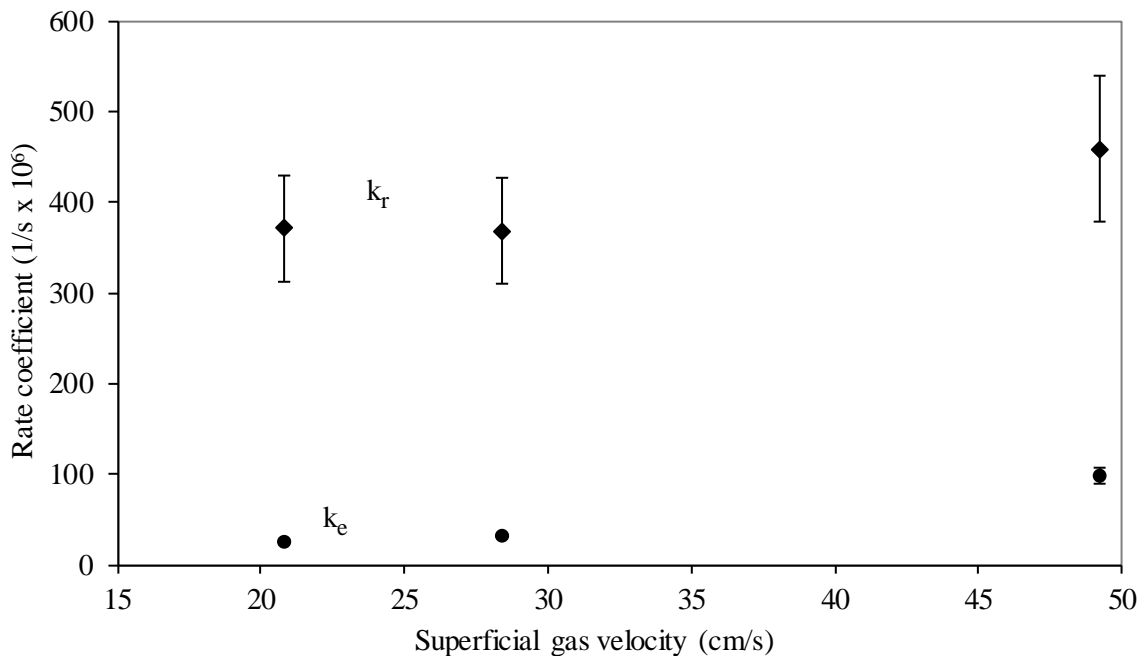
237
 238 Figure 4. Comparison between experimental char carbon loadings in the reactor and model predictions at
 239 various times for gasification of fine ground seed corn at 715°C and two ER values (0.27 and 0.31). Data
 240 shown is for experiments *a-j*.
 241

242 4.3.1 Effect of the superficial gas velocity

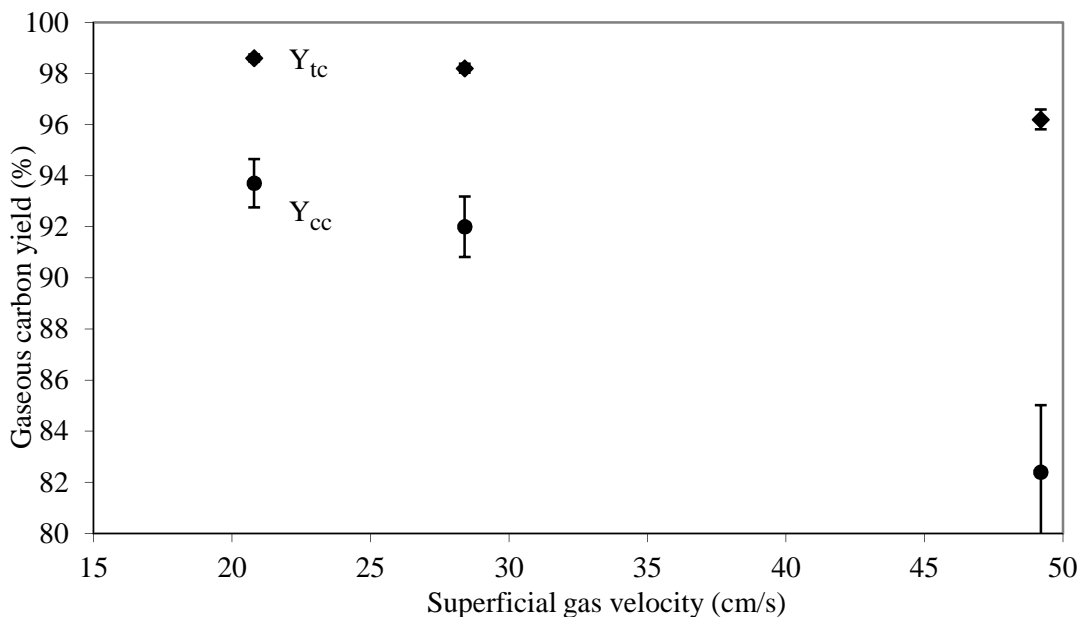
243 Superficial gas velocity was varied by changing the air supply rate and adjusting the biomass feed
 244 rate to achieve similar ER values across the experiments. Figure 5 plots k_r and k_c as functions of the
 245 superficial gas velocity, U_{fb} , in the reactor during gasification of ground seed corn at 750°C with an ER of
 246 0.29 (Experiments *k, l, m*). The absence of much effect of superficial gas velocity on k_r demonstrated that
 247 gasification of ground seed corn at these conditions was not limited by mass transfer from the bulk fluid
 248 to the char particles, which is consistent with the findings of others [7], [24], [52]–[58]. The increasing
 249 trend of k_c with increasing superficial gas velocities shown in Figure 5 was expected as larger particles
 250 became elutriable and physical attrition increased [47], [59].

251 Increasing superficial gas velocity increased char elutriation rates but did not increase chemical
 252 reaction rates beyond the uncertainty in the data, resulting in a decrease in both Y_{tc} (Eq. (9)) and Y_{cc} (Eq.
 253 (12)), as shown in Figure 6. Conversely, gas carbon yield increased as superficial gas velocity was

254 reduced. In other words, increasing the diameter of the gasifier for a given biomass feed rate should
 255 achieve low char elutriation rates and correspondingly higher gas carbon yields.



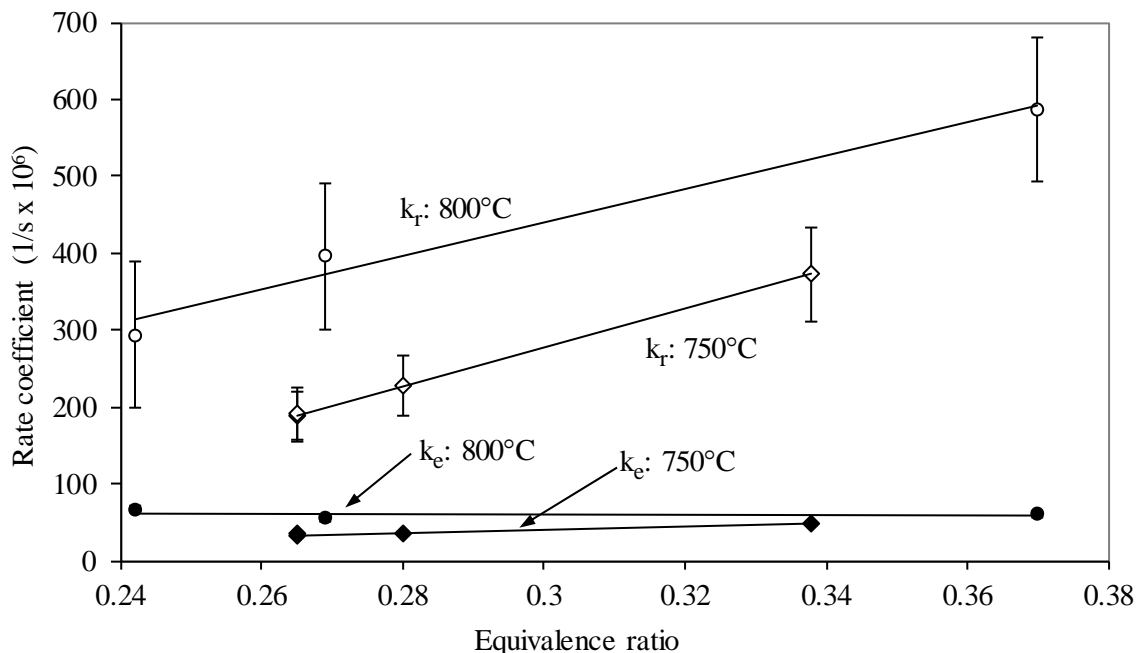
256
 257 Figure 5. Rate coefficient for char carbon conversion and elutriation as a function of the superficial gas
 258 velocity during gasification of fine ground seed corn at approximately 750°C and an ER of 0.29. Data
 259 from experiments *k*, *l*, and *m*.
 260



261
 262 Figure 6. Total carbon gas yield from biomass and carbon gas yield from char carbon as a function of
 263 superficial gas velocity during gasification of fine ground seed corn at approximately 750°C and an ER of
 264 0.29. Data from experiments *k*, *l*, and *m*.
 265

266 4.3.2 Effect of equivalence ratio

267 Rate coefficients for chemical reaction and elutriation during gasification of ground seed corn at
268 750°C and 800°C are plotted as functions of equivalence ratio in Figure 7 (Experiments n – t). ER values
269 were varied by altering the biomass feed rate while maintaining a constant air flow rate of 50 slpm.
270 Linear regression lines were added to the figure for clarity. Both temperatures show k_r increasing linearly
271 with increased ER as a result of increased char oxidation.



272
273 Figure 7. Rate coefficient for char carbon conversion and elutriation as a function of ER for gasification
274 of fine ground seed corn at approximately 750°C and 800°C. Data from experiments n – t.
275

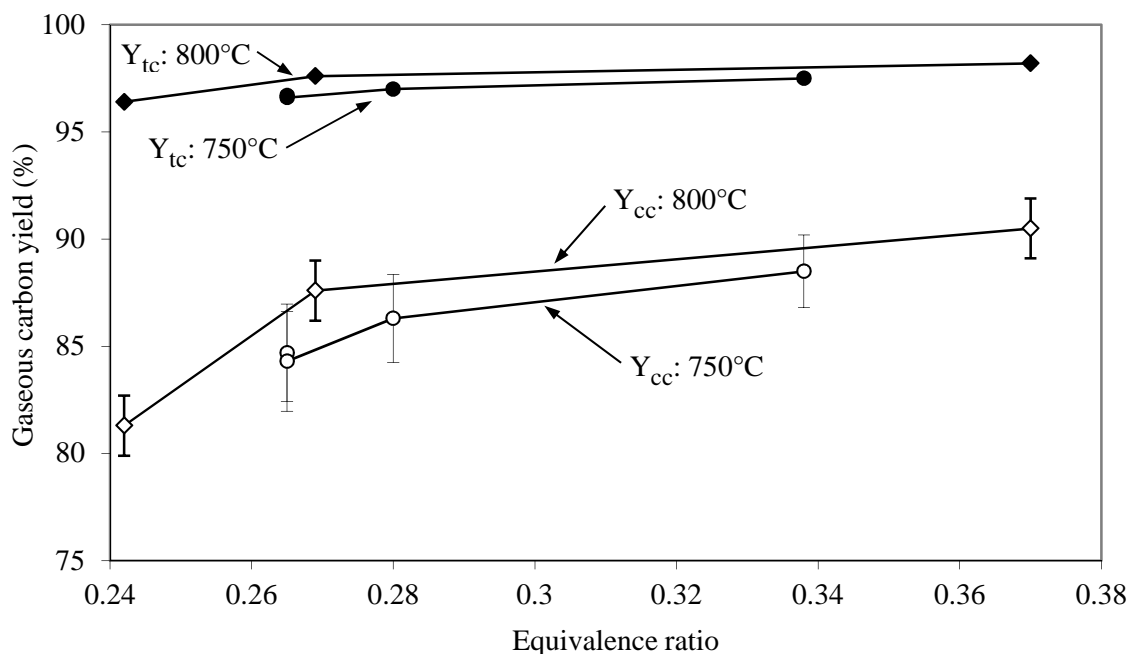
276 During these tests superficial gas velocity in the gasifier decreased as equivalence ratio was increased.
277 This was result of the corresponding lower biomass feed rates generating smaller volumes of volatile
278 gases and vapors. Elutriation rate coefficient was expected to decrease with reductions in the superficial
279 gas velocity in accordance with the trend demonstrated in Figure 5. However, despite a 10-20% decrease
280 in superficial gas velocity with increased ER, elutriation rate coefficients plotted in Figure 7 are constant
281 or increase only slightly. Increasing elutriation rates with increasing ER despite decreasing superficial
282 gas velocity indicates the presence of increasing rates of chemically enhanced attrition. Chemically
283 enhanced attrition is a form of percolation in which chemical conversion weakens the char particles

284 making them more susceptible to physical attrition. Scala *et al.* [60], [61] observed this phenomena
285 during combustion of black locust char.

286 Steam and CO₂ gasification reactions are endothermic and are therefore expected to increase with
287 temperature. Figure 7 is consistent with this expectation showing larger k_r values at 800°C compared to
288 750°C regardless of ER.

289 Figure 7 also shows a larger elutriation rate coefficient for gasification at 800°C than at 750°C,
290 consistent with increased chemically enhanced attrition due to the increased chemical conversion
291 experienced at higher temperatures. However, the data are not conclusive in this case as the increased
292 elutriation may be the result of higher superficial gas velocity due to increased volatiles release as
293 temperature increases.

294 Gas carbon yield from char, Y_{cc} (Eq. (12)), and total gas carbon yield from biomass, Y_{tc} (Eq. (9)), are
295 plotted as functions of ER in Figure 8. As expected, increased carbon gas yield from char and total
296 carbon gas yield were realized with increased equivalence ratio for both gasification temperatures.

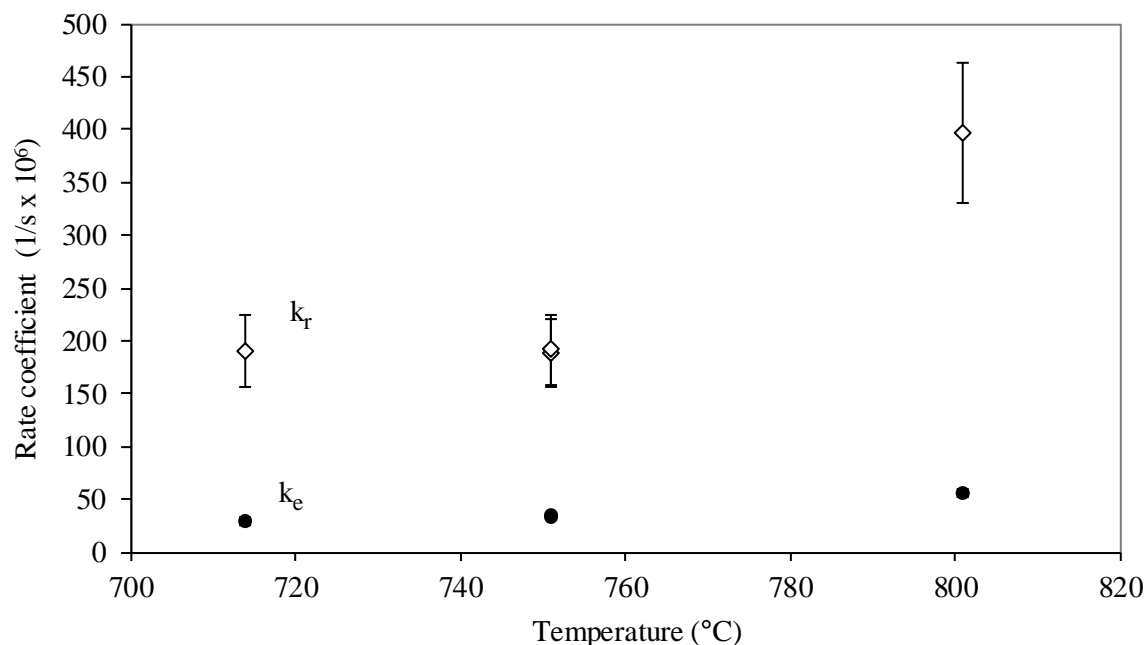


297
298 Figure 8. Total carbon gas yield (Y_{tc}) from biomass and carbon gas yield (Y_{cc}) from char carbon as a
299 function of ER for gasification of fine ground seed corn at approximately 750°C and 800°C. Data from
300 experiments $n - t$)
301

302 Consistent with published data for various types of biomass [1], [9], [11]–[15], [21], [23], [26], the
303 results of this study show increased carbon gas yield with increased equivalence ratios. Carbon balance
304 analysis revealed chemical reaction rates increased linearly with increased ER over the ranges tested. The
305 analysis also showed steady or slightly increasing elutriation rates with increased ER in spite of
306 decreasing reactor gas velocities. This suggests that chemically enhanced attrition may have been active
307 during gasification of ground seed corn, limiting the yield of carbon bearing gases.

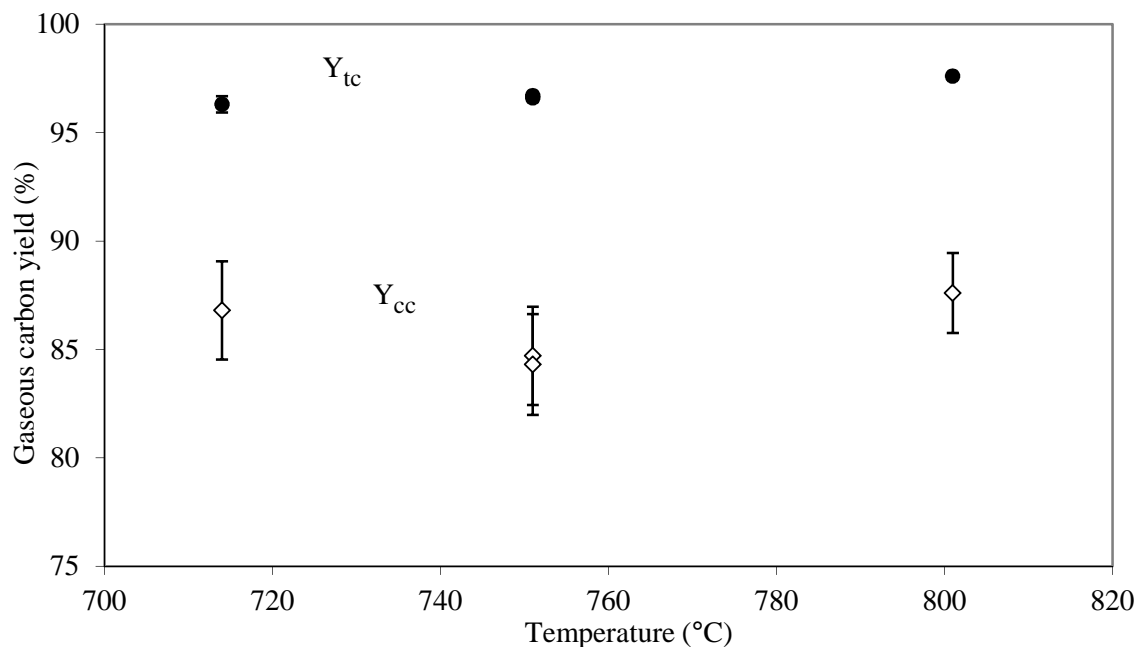
308 4.3.3 Effect of temperature

309 Figure 9 plots k_r and k_e as a function of temperature for the gasification of ground seed corn
310 (Experiments *j*, *o*, *q*, *r*). The figure shows a large increase in the chemical reaction rate coefficient with
311 temperature as well as an increase in the elutriation rate coefficient. Whether this increase in elutriation
312 was caused by increased chemically enhanced attrition, increased fragmentation during devolatilization
313 due to the higher temperature [26], [62], [63], increased superficial gas velocity arising from higher
314 temperatures, or some combination of these factors, was not discernable from this data.



315 Figure 9. Rate coefficient for char carbon conversion and elutriation as functions of temperature for the
316 gasification of fine ground seed corn at an average ER of 0.27. Data from experiments *j*, *o*, *q*, *r*.
317
318

319 Figure 10 plots carbon gas yield as a function of gasification temperature. Within the uncertainties of
 320 the data the figure shows little or no change in Y_{cc} across the entire temperature range and only a modest
 321 increase in Y_{tc} due in part to the additional volatile release experienced at the higher temperatures [32],
 322 [34], [41]–[45], [51]. Therefore, despite the fact that the chemical conversion per unit mass of char
 323 carbon doubles over the range of temperature tested, a near doubling of the elutriation rate prevented a
 324 significant increase in the carbon gas yield. The lack of improved carbon gas yield with increased
 325 temperature shown in this study is a trend that has been observed by others but not completely explained
 326 [1], [13], [14], [16], [17], [19], [20]. In this study the benefit of increased chemical reaction rates due to
 327 higher temperatures was offset by increased elutriation of carbon. Although other potential mechanisms
 328 cannot be ruled out based on the data, this result is consistent with the explanation that carbon gas yield
 329 was not limited by either mass transport or chemical kinetics but by chemically enhanced attrition of the
 330 char, which increased with temperature and the corresponding increased chemical reaction rates.



331 Figure 10. Total carbon gas yield from biomass and carbon gas yield from char carbon as functions of
 332 temperature for gasification of fine ground seed corn at an average ER of 0.27. Data from experiments j , o ,
 333 q , r .
 334
 335

336 *4.3.4 Effect of biomass particle size*

337 The gasification behavior of fine and coarse seed corn particles was compared. Based on sieve data
 338 the average mass weighted diameter was 0.96 mm for the fine ground seed corn and 1.9 mm for the
 339 coarse. Table 3 summarizes the results for gasification experiments at 750°C, ER = 0.28 and 800°C, ER
 340 = 0.27 (Experiments *o*, *s*, *u*, *v*). For each temperature the data show increased elutriation rates for coarse
 341 particles compared to fine particles while chemical reaction rates were similar. As the size of biomass
 342 particles increases the likelihood of fragmentation during devolatilization also increases [62], [63]. The
 343 increase in char surface area realized from increased fragmentation did not lead to an increase in chemical
 344 reaction rate coefficient because, as shown earlier (see *Section 4.3.1*), in these experiments reaction rates
 345 were not limited by mass transfer from the bulk fluid to the char particle. Additionally, it is likely that
 346 many of the fragments were of elutriable size and left the reactor after being formed with little time for
 347 chemical reaction, resulting in the increased elutriation rates for the coarse fuel particles shown in the
 348 table. Table 3 also shows a decrease in Y_{cc} and Y_{tc} as the particle size was increased, which is consistent
 349 with trends observed by Nikoo and Mahinpey [30]. The decrease in carbon gas yield observed here was
 350 expected given the higher elutriation rates and similar chemical reaction rates for coarse corn compared to
 351 the fine.

352 Table 3. Ground seed corn gasification data used to analyze the effect of biomass particle size

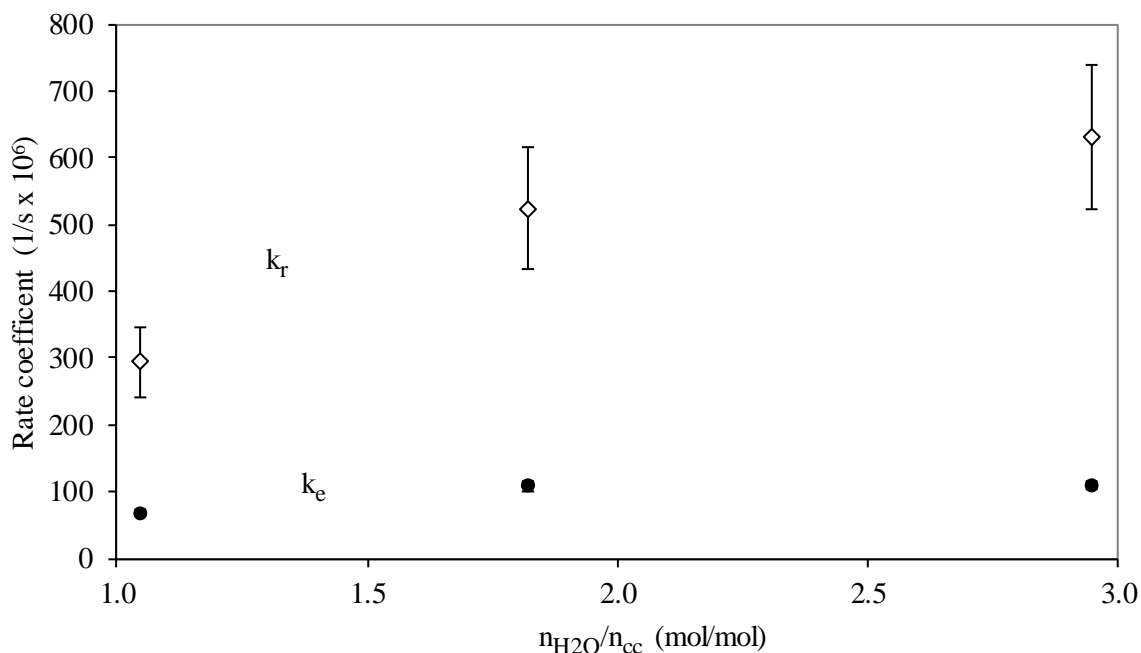
Experiment	Temp (°C)	ER	n_{H_2O}/n_{cc} (mol/mol)	U_{fb} (cm/s)	Biomass Size	k_r ($\times 10^6 s^{-1}$)	k_e ($\times 10^6 s^{-1}$)	Y_{cc} (%)	Y_{tc} (%)
<i>s</i>	753	0.28	0.9±0.15	30±1	Fine	230±40	36±2	86±2	97.0±0.2
<i>u</i>	746	0.28	0.9±0.15	26±1	Coarse	210±40	46±3	82±3	95.9±0.2
<i>o</i>	801	0.27	1.0±0.15	35±1	Fine	400±70	56±4	88±2	97.6±0.1
<i>v</i>	801	0.27	1.0±0.15	34±1	Coarse	350±70	97±6	78±4	95.8±0.2

354 4.3.5 Effect of H_2O concentration

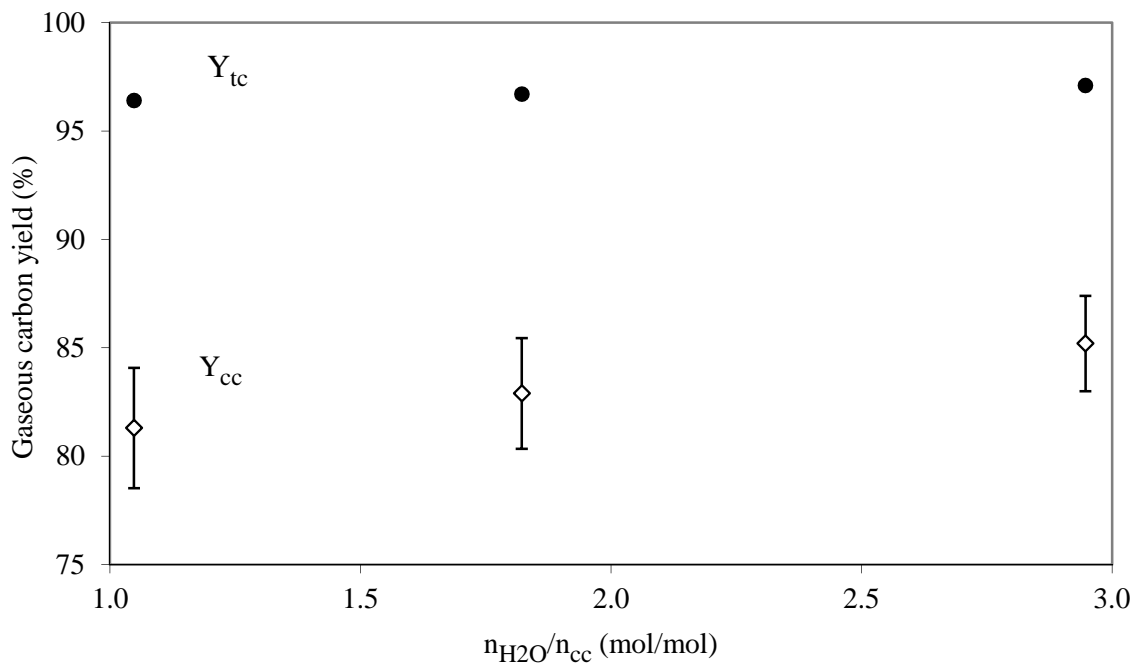
355 Moisture in the ground seed corn provided a molar ratio of water vapor to char carbon (n_{H_2O}/n_{cc}) of
 356 1.0 during gasification at 800°C. This ratio was increased by injecting wet steam into the bottom of the
 357 fluidized bed to achieve n_{H_2O}/n_{cc} as high as 2.9.

358 Figure 11 shows a significant increase in k_r and k_e as n_{H_2O}/n_{cc} increased (Experiments *n*, *w*, *x*).
 359 Similar to the result observed for temperature (see *Section 4.3.3*), increased chemical reaction rates

360 corresponded to increased elutriation rates, indicating the presence of chemically enhanced attrition.
 361 When chemically enhanced attrition is operative, increased chemical reaction is offset by increased char
 362 elutriation leaving carbon gas yields essentially unchanged as shown in Figure 12. The figure shows a
 363 slight increase in Y_{tc} and no significant change in Y_{cc} beyond uncertainty in the data as n_{H_2O}/n_{cc}
 364 increased from 1.0 to nearly 3.0. Thus, while the addition of H_2O may be desirable for reforming tar or to
 365 increase H_2 concentrations via the water-gas shift reaction [16], [20], [21], [31], [43], [64], it did not
 366 improve the yield of carbon bearing gases in these experiments.



367
 368 Figure 11. Rate coefficient for char carbon conversion and elutriation as functions of the water vapor
 369 concentration per mole of char carbon entering the reactor during gasification of fine ground seed corn at
 370 approximately 800°C, ER = 0.25. Data from experiments n , w , x .
 371



372
 373 Figure 12. Total carbon gas yield from biomass and carbon gas yield from char carbon as a function of
 374 the water vapor concentration per mole of char carbon entering the reactor during gasification of fine
 375 ground seed corn at approximately 800°C, ER = 0.25. Data from experiments *n*, *w*, *x*.
 376

377 5. Conclusions

378 A char carbon balance on a fluidized bed gasifier was used to better understand the conversion of char
 379 carbon to carbon bearing gases. In experiments with ground seed corn, it was found that the yield of
 380 carbon bearing gases was often limited by chemically enhanced attrition of the char particles. Therefore,
 381 efforts to improve carbon gas yield by increasing chemical reaction rates are frustrated by increased
 382 elutriation rates from chemically enhanced attrition. These results explain why previous studies found
 383 little improvement in carbon gas yield when operating under conditions that increased the rate of solid-
 384 gas reactions of char. The most promising strategy to improve yields of carbon-bearing gases during
 385 fluidized bed gasification of biomass is to reduce superficial gas velocity, which decreases char attrition
 386 while maintaining the rate of gas-solid reactions.

387

388 Acknowledgements

389 This work was supported by the Natural Resources Conservation Service, U. S. Department of
390 Agriculture under Agreement No. NRCS 68-3-475-3151; the U. S. Department of Energy under
391 Agreement No. DE-FC36-01G011091; and the ISU Foundation under the Bergles Professorship in
392 Thermal Sciences at Iowa State University. Any opinions, findings, conclusions, or recommendations
393 expressed herein are those of the authors and do not necessarily reflect the views of the sponsors.

394 **References**

- 395 [1] X. T. Li, J. R. Grace, C. J. Lim, A. P. Watkinson, H. P. Chen, and J. R. Kim, "Biomass gasification
396 in a circulating fluidized bed," *Biomass Bioenergy*, vol. 26, no. 2, pp. 171–193, 2004.
- 397 [2] C. M. Kinoshita, Y. Wang, and P. K. Takahashi, "Chemical equilibrium computations for
398 gasification of biomass to produce methanol," *Energy Sources*, vol. 13, no. 3, pp. 361–368, 1991.
- 399 [3] X. Li, J. R. Grace, A. P. Watkinson, C. J. Lim, and A. Ergüdenler, "Equilibrium modeling of
400 gasification: a free energy minimization approach and its application to a circulating fluidized bed
401 coal gasifier," *Fuel*, vol. 80, no. 2, pp. 195–207, 2001.
- 402 [4] M. J. Prins, K. J. Ptasiński, and F. Janssen, "Thermodynamics of gas-char reactions: first and second
403 law analysis," *Chem. Eng. Sci.*, vol. 58, no. 3, pp. 1003–1011, 2003.
- 404 [5] M. Ruggiero and G. Manfredi, "An equilibrium model for biomass gasification processes," *Renew.
405 Energy*, vol. 16, no. 1–4, pp. 1106–1109, 1999.
- 406 [6] G. Schuster, G. Löffler, K. Weigl, and H. Hofbauer, "Biomass steam gasification—an extensive
407 parametric modeling study," *Bioresour. Technol.*, vol. 77, no. 1, pp. 71–79, 2001.
- 408 [7] T. B. Reed editor, *Biomass Gasification: Principles and Technology*, Solar Energy Research
409 Institute, Noyes Data Corp., Park Ridge, N.J., 1981.
- 410 [8] M. Baratieri, P. Baggio, L. Fiori, and M. Grigiante, "Biomass as an energy source: Thermodynamic
411 constraints on the performance of the conversion process," *Bioresour. Technol.*, vol. 99, no. 15, pp.
412 7063–7073, Oct. 2008.
- 413 [9] L. Zeng and A. R. Van Heiningen, "Carbon gasification of kraft black liquor solids in the presence
414 of TiO₂ in a fluidized bed," *Energy Fuels*, vol. 14, no. 1, pp. 83–88, 2000.
- 415 [10] P. Garcia-Ibanez, A. Cabanillas, and J. M. Sánchez, "Gasification of leached orujillo (olive oil
416 waste) in a pilot plant circulating fluidised bed reactor. Preliminary results," *Biomass Bioenergy*, vol.
417 27, no. 2, pp. 183–194, 2004.
- 418 [11] A. Gómez-Barea, R. Arjona, and P. Ollero, "Pilot-plant gasification of olive stone: a technical
419 assessment," *Energy Fuels*, vol. 19, no. 2, pp. 598–605, 2005.
- 420 [12] S. R. Kersten, W. Prins, A. Van der Drift, and W. P. M. van Swaaij, "Experimental fact-finding in
421 CFB biomass gasification for ECN's 500 kWth pilot plant," *Ind. Eng. Chem. Res.*, vol. 42, no. 26,
422 pp. 6755–6764, 2003.
- 423 [13] P. M. Lv, Z. H. Xiong, J. Chang, C. Z. Wu, Y. Chen, and J. X. Zhu, "An experimental study on
424 biomass air–steam gasification in a fluidized bed," *Bioresour. Technol.*, vol. 95, no. 1, pp. 95–101,
425 2004.
- 426 [14] F. Miccio, O. Moersch, H. Spliethoff, and K. R. G. Hein, "Generation and conversion of
427 carbonaceous fine particles during bubbling fluidised bed gasification of a biomass fuel," *Fuel*, vol.
428 78, no. 12, pp. 1473–1481, 1999.
- 429 [15] A. van der Drift and J. van Doorn, "Effect of fuel size and process temperature on fuel gas quality
430 from CFB gasification of biomass," *Prog. Thermochem. Biomass Convers.*, p. 265, 2008.
- 431 [16] J. Herguido, J. Corella, and J. Gonzalez-Saiz, "Steam gasification of lignocellulosic residues in a
432 fluidized bed at a small pilot scale. Effect of the type of feedstock," *Ind. Eng. Chem. Res.*, vol. 31,
433 no. 5, pp. 1274–1282, 1992.

- 434 [17] A. van der Drift, J. van Doorn, and J. W. Vermeulen, "Ten residual biomass fuels for circulating
435 fluidized-bed gasification," *Biomass Bioenergy*, vol. 20, no. 1, pp. 45–56, 2001.
- 436 [18] A. van der Drift and C. M. van der Meijden, "Ways to increase the carbon conversion of a CFB
437 gasifier," in *12th European Conference and Exhibition on Biomass for Energy and Climate
438 Protection*, Amsterdam, 2002, p. 48.
- 439 [19] C. Franco, F. Pinto, I. Gulyurtlu, and I. Cabrita, "The study of reactions influencing the biomass
440 steam gasification process," *Fuel*, vol. 82, no. 7, pp. 835–842, 2003.
- 441 [20] J. Gil, M. P. Aznar, M. A. Caballero, E. Francés, and J. Corella, "Biomass gasification in fluidized
442 bed at pilot scale with steam-oxygen mixtures. Product distribution for very different operating
443 conditions," *Energy Fuels*, vol. 11, no. 6, pp. 1109–1118, 1997.
- 444 [21] M. Campoy, A. Gómez-Barea, A. L. Villanueva, and P. Ollero, "Air–Steam Gasification of
445 Biomass in a Fluidized Bed under Simulated Autothermal and Adiabatic Conditions," *Ind. Eng.
446 Chem. Res.*, vol. 47, no. 16, pp. 5957–5965, Aug. 2008.
- 447 [22] J. Kramb, J. Kontinen, A. Gómez-Barea, A. Moilanen, and K. Umeki, "Modeling biomass char
448 gasification kinetics for improving prediction of carbon conversion in a fluidized bed gasifier," *Fuel*,
449 vol. 132, pp. 107–115, Sep. 2014.
- 450 [23] A. Kumar, K. Eskridge, D. D. Jones, and M. A. Hanna, "Steam–air fluidized bed gasification of
451 distillers grains: Effects of steam to biomass ratio, equivalence ratio and gasification temperature,"
452 *Bioresour. Technol.*, vol. 100, no. 6, pp. 2062–2068, Mar. 2009.
- 453 [24] M. Campoy, A. Gómez-Barea, F. B. Vidal, and P. Ollero, "Air–steam gasification of biomass in a
454 fluidised bed: Process optimisation by enriched air," *Fuel Process. Technol.*, vol. 90, no. 5, pp. 677–
455 685, May 2009.
- 456 [25] A. Gómez-Barea, B. Leckner, A. Villanueva Perales, S. Nilsson, and D. Fuentes Cano, "Improving
457 the performance of fluidized bed biomass/waste gasifiers for distributed electricity: A new three-
458 stage gasification system," *Appl. Therm. Eng.*, vol. 50, no. 2, pp. 1453–1462, Feb. 2013.
- 459 [26] A. Gómez-Barea and B. Leckner, "Estimation of gas composition and char conversion in a fluidized
460 bed biomass gasifier," *Fuel*, vol. 107, pp. 419–431, May 2013.
- 461 [27] A. Gómez-Barea, P. Ollero, and B. Leckner, "Optimization of char and tar conversion in fluidized
462 bed biomass gasifiers," *Fuel*, vol. 103, pp. 42–52, Jan. 2013.
- 463 [28] S. Kaewluan and S. Pipatmanomai, "Potential of synthesis gas production from rubber wood chip
464 gasification in a bubbling fluidised bed gasifier," *Energy Convers. Manag.*, vol. 52, no. 1, pp. 75–84,
465 Jan. 2011.
- 466 [29] D. Neves, H. Thunman, A. Matos, L. Tarelho, and A. Gómez-Barea, "Characterization and
467 prediction of biomass pyrolysis products," *Prog. Energy Combust. Sci.*, vol. 37, no. 5, pp. 611–630,
468 Sep. 2011.
- 469 [30] M. B. Nikoo and N. Mahinpey, "Simulation of biomass gasification in fluidized bed reactor using
470 ASPEN PLUS," *Biomass Bioenergy*, vol. 32, no. 12, pp. 1245–1254, Dec. 2008.
- 471 [31] I. Narvaez, A. Orió, M. P. Aznar, and J. Corella, "Biomass gasification with air in an atmospheric
472 bubbling fluidized bed. Effect of six operational variables on the quality of the produced raw gas,"
473 *Ind. Eng. Chem. Res.*, vol. 35, no. 7, pp. 2110–2120, 1996.
- 474 [32] C. Hanping, L. Bin, Y. Haiping, Y. Guolai, and Z. Shihong, "Experimental Investigation of
475 Biomass Gasification in a Fluidized Bed Reactor," *Energy Fuels*, vol. 22, no. 5, pp. 3493–3498, Sep.
476 2008.
- 477 [33] V. Sricharoenchaikul, W. J. Frederick, and P. Agrawal, "Carbon distribution in char residue from
478 gasification of kraft black liquor," *Biomass Bioenergy*, vol. 25, no. 2, pp. 209–220, 2003.
- 479 [34] D. S. Scott, J. Piskorz, M. A. Bergougnou, R. Graham, and R. P. Overend, "The role of temperature
480 in the fast pyrolysis of cellulose and wood," *Ind. Eng. Chem. Res.*, vol. 27, no. 1, pp. 8–15, 1988.
- 481 [35] C. Sheng and J. L. T. Azevedo, "Modeling biomass devolatilization using the chemical percolation
482 devolatilization model for the main components," *Proc. Combust. Inst.*, vol. 29, no. 1, pp. 407–414,
483 2002.

- 484 [36] V. Cozzani, C. Nicolella, M. Rovatti, and L. Tognotti, "Modeling and experimental verification of
485 physical and chemical processes during pyrolysis of a refuse-derived fuel," *Ind. Eng. Chem. Res.*,
486 vol. 35, no. 1, pp. 90–98, 1996.
- 487 [37] V. Sricharoenchaikul, A. L. Hicks, and W. J. Frederick, "Carbon and char residue yields from rapid
488 pyrolysis of kraft black liquor," *Bioresour. Technol.*, vol. 77, no. 2, pp. 131–138, 2001.
- 489 [38] X. Bingyan, W. Chuangzhi, L. Zhengfen, and others, "Kinetic study on biomass gasification (A
490 1991 ISES Solar World Congress honors paper)," *Sol. Energy*, vol. 49, no. 3, pp. 199–204, 1992.
- 491 [39] W. J. Frederick Jr and M. Hupa, "Combustion properties of kraft black liquors," USDOE Assistant
492 Secretary for Energy Efficiency and Renewable Energy, Washington, DC (United States). Office of
493 Industrial Technologies; Tampella Power, Tampere (Finland); Ministry of Trade and Industry,
494 Helsinki (Finland). Energy Dept.; Oregon State Univ., Corvallis, OR (United States); Aabo
495 Akademi, Turku (Finland), 1993.
- 496 [40] P. Mathieu and R. Dubuisson, "Performance analysis of a biomass gasifier," *Energy Convers.*
497 *Manag.*, vol. 43, no. 9, pp. 1291–1299, 2002.
- 498 [41] R. Zanzi, K. Sjöström, and E. Björnbom, "Rapid pyrolysis of agricultural residues at high
499 temperature," *Biomass Bioenergy*, vol. 23, no. 5, pp. 357–366, 2002.
- 500 [42] S. Gaur and T. B. Reed, *Thermal data for natural and synthetic fuels*. Marcel Dekker New York,
501 1998.
- 502 [43] A. Gómez-Barea, B. Leckner, and P. Ollero, "Methods to improve the performance of fluidized bed
503 biomass gasifiers," in *2nd European conference on polygeneration, Tarragona (Spain)*, 2011.
- 504 [44] D. Fuentes-Cano, A. Gómez-Barea, S. Nilsson, and P. Ollero, "The influence of temperature and
505 steam on the yields of tar and light hydrocarbon compounds during devolatilization of dried sewage
506 sludge in a fluidized bed," *Fuel*, vol. 108, pp. 341–350, Jun. 2013.
- 507 [45] A. Gomez-Barea, S. Nilsson, F. Vidal Barrero, and M. Campoy, "Devolatilization of wood and
508 wastes in fluidized bed," *Fuel Process. Technol.*, vol. 91, no. 11, pp. 1624–1633, Nov. 2010.
- 509 [46] R. C. Brown, J. Ahrens, and N. Christofides, "The contributions of attrition and fragmentation to
510 char elutriation from fluidized beds," *Combust. Flame*, vol. 89, no. 1, pp. 95–102, 1992.
- 511 [47] D. Harrison, R. Clift, and J. F. Davidson, *Fluidization*, 2nd ed. London: Academic Press, 1985.
- 512 [48] S. Q. Turn, C. M. Kinoshita, D. M. Ishimura, and J. Zhou, "The fate of inorganic constituents of
513 biomass in fluidized bed gasification," *Fuel*, vol. 77, no. 3, pp. 135–146, 1998.
- 514 [49] A. Olivares, M. P. Aznar, M. A. Caballero, J. Gil, E. Francés, and J. Corella, "Biomass gasification:
515 produced gas upgrading by in-bed use of dolomite," *Ind. Eng. Chem. Res.*, vol. 36, no. 12, pp.
516 5220–5226, 1997.
- 517 [50] H.W. Coleman, W. G. Steele, *Experimentation, Validation, and Uncertainty Analysis for Engineers*,
518 3rd Edition, New York: Wiley, 2009.
- 519 [51] R. Zanzi, K. Sjöström, and E. Björnbom, "Rapid high-temperature pyrolysis of biomass in a free-
520 fall reactor," *Fuel*, vol. 75, no. 5, pp. 545–550, 1996.
- 521 [52] R. Backman, W. J. Frederick, and M. Hupa, "Basic studies on black-liquor pyrolysis and char
522 gasification," *Bioresour. Technol.*, vol. 46, no. 1–2, pp. 153–158, 1993.
- 523 [53] U. B. Desideri N. . and D. Fiaschi, "A biomass combustion-gasification model: validation and
524 sensitivity analysis," *J. Energy Resour. Technol.*, vol. 117, p. 329, 1995.
- 525 [54] P. Ollero, A. Serrera, R. Arjona, and S. Alcantarilla, "The CO₂ gasification kinetics of olive
526 residue," *Biomass Bioenergy*, vol. 24, no. 2, pp. 151–161, 2003.
- 527 [55] R. H. Hurt, "Structure, properties, and reactivity of solid fuels," in *Symposium (International) on*
528 *Combustion*, 1998, vol. 27, pp. 2887–2904.
- 529 [56] W. Klose and M. Wölki, "On the intrinsic reaction rate of biomass char gasification with carbon
530 dioxide and steam," *Fuel*, vol. 84, no. 7, pp. 885–892, 2005.
- 531 [57] E. Henrich, S. Bürkle, Z. I. Meza-Renken, and S. Rumpel, "Combustion and gasification kinetics of
532 pyrolysis chars from waste and biomass," *J. Anal. Appl. Pyrolysis*, vol. 49, no. 1, pp. 221–241, 1999.
- 533 [58] T. Kojima, P. Assavadakorn, and T. Furusawa, "Measurement and evaluation of gasification
534 kinetics of sawdust char with steam in an experimental fluidized bed," *Fuel Process. Technol.*, vol.
535 36, no. 1–3, pp. 201–207, 1993.

- 536 [59] Y. Chen, Handbook of fluidization and fluid-particle systems. Marcel Dekker New York, 2003.
- 537 [60] F. Scala, P. Salatino, and R. Chirone, "Fluidized bed combustion of a biomass char (*Robinia*
- 538 *pseudoacacia*)," *Energy Fuels*, vol. 14, no. 4, pp. 781–790, 2000.
- 539 [61] F. Scala and R. Chirone, "Fluidized bed combustion of alternative solid fuels," *Exp. Therm. Fluid*
- 540 *Sci.*, vol. 28, no. 7, pp. 691–699, 2004.
- 541 [62] F. Scala, R. Chirone, and P. Salatino, "Combustion and attrition of biomass chars in a fluidized bed,"
- 542 *Energy Fuels*, vol. 20, no. 1, pp. 91–102, 2006.
- 543 [63] N. Jand and P. U. Foscolo, "Decomposition of wood particles in fluidized beds," *Ind. Eng. Chem.*
- 544 *Res.*, vol. 44, no. 14, pp. 5079–5089, 2005.
- 545 [64] J. Gil, J. Corella, M. P. Aznar, and M. A. Caballero, "Biomass gasification in atmospheric and
- 546 bubbling fluidized bed: effect of the type of gasifying agent on the product distribution," *Biomass*
- 547 *Bioenergy*, vol. 17, no. 5, pp. 389–403, 1999.
- 548